



## Near-infrared reflection spectroscopy (NIRS) as a successful tool for simultaneous identification and particle size determination of amoxicillin trihydrate

L.K.H. Bittner<sup>a</sup>, N. Heigl<sup>a</sup>, C.H. Petter<sup>a</sup>, M.F. Noisternig<sup>b</sup>, U.J. Griesser<sup>b</sup>, G.K. Bonn<sup>a</sup>, C.W. Huck<sup>a,\*</sup>

<sup>a</sup> Institute of Analytical Chemistry and Radiochemistry, Leopold-Franzens University, Innrain 52a, 6020 Innsbruck, Austria

<sup>b</sup> Institute of Pharmacy, Leopold-Franzens University, Innrain 52, 6020 Innsbruck, Austria

### ARTICLE INFO

#### Article history:

Received 20 October 2010

Received in revised form

12 December 2010

Accepted 15 December 2010

Available online 22 December 2010

#### Keywords:

Near infrared spectroscopy

Amoxicillin

Particle size

Fractionation

Beta-lactam antibiotic

### ABSTRACT

A successful application of NIR spectroscopy (NIRS) in combination with multivariate data analysis (MVA) for the simultaneous identification and particle size determination of amoxicillin trihydrate particles was developed. Particle size analysis was ascertained by NIRS in diffuse reflection mode on different particle size fractions of amoxicillin trihydrate with D90 particle diameters ranging from 6.9 to 21.7  $\mu\text{m}$ . The present problem of fractionating the powder into good enough size fractions to achieve a stable calibration model was solved. By probing dried suspensions measurement parameters were optimized and further combined with the best suitable chemometric operations. Thereby the quality of established regression models could be improved considerably. A linear coherence between particle size and absorbance signal was found at specific wavenumbers. Satisfactory clustering by particle size was achieved by principal component analysis (PCA) whereas partial least squares regression (PLSR) and principal component regression (PCR) was compared for quantitatively calibrating the NIRS data. PLSR turned out to predict unknown test samples slightly better than PCR.

© 2010 Elsevier B.V. All rights reserved.

### 1. Introduction

Amoxicillin trihydrate, its chemical structure is shown in Fig. 1, is an orally administered, broad-spectrum,  $\beta$ -lactam antibiotic. It belongs to the most prescribed drugs and is produced on a large scale worldwide. The adjustment and control of the particle size of the active pharmaceutical ingredient is crucial for a variety of steps in the manufacturing processes of a solid fast-releasing drug product and one of the most critical parameters with regard to an acceptable drug performance. Conventional methods such as sieve analysis or image analysis are rather time-consuming and hard to automate. Today, laser diffraction is the most commonly applied particle sizing technique that allows also on-line measurements in industrial manufacturing processes. Since this method is rapid, requires a small volume, provides information about particle size distribution, does not need an external calibration, shows high reproducibility and can perform in a wet and dry medium, laser diffraction is regarded as the gold standard in particle size analysis. Near-infrared-spectroscopy (NIRS) combined with multivariate data analysis (MVA) represents the most recent approach in particle size analysis. The method offers a powerful, fast, easy-to-handle, high-throughput and non-destructive analytical tool while hardly any sample preparation is necessary. Moreover NIRS offers the pos-

sibility for on- and in-line real-time monitoring of processes. This feature makes NIRS one of the most attractive methods for the process analytical technology (PAT) initiative of the US Food and Drug Administration (FDA), which aims to “design the quality” of a product by monitoring and optimizing the production process instead of exclusively evaluating the quality of the final product in quality control laboratories [1]. For qualitative and quantitative analysis MVA-based calibration techniques are used to correlate the spectroscopic data with the data obtained by reference techniques. In this context preferably principal component analysis (PCA) based algorithms like principal component regression (PCR) or partial least squares regression (PLSR) are applied [2–5].

To achieve a stable calibration it is necessary to investigate a number of different samples covering a broad range of the property which should be predicted. Thus well-defined particle size fractions of amoxicillin trihydrate were prepared to establish a suitable calibration set.

Numerous spectra pretreatments are available to increase the prediction ability of the established calibrations. Most of them focus on the elimination of baseline offsets caused by scattering effects. Results obtained from NIR-measurements can, in some cases, offer even more precise analytical data than a particular reference method. This may be the case if the calibration is based on a large number of samples to reduce the random errors of the reference method [6].

It is well known that particle size affects the characteristics of NIR diffuse reflection spectra [7]. Usually this effect can be observed

\* Corresponding author. Tel.: +43 512 507 5195; fax: +43 512 507 2965.

E-mail address: [Christian.W.Huck@uibk.ac.at](mailto:Christian.W.Huck@uibk.ac.at) (C.W. Huck).

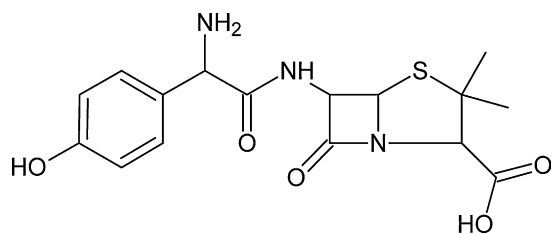


Fig. 1. Chemical structure of amoxicillin.

as an offset (parallel shift) of the baseline [8]. Kubelka described the light-scattering of solid samples already in 1948 [9]. Years before he and Munk developed a model relating the reflectance ( $R$ ) to the scattering coefficient ( $S$ ) and the absorption coefficient ( $K$ ), which is known as the so-called Kubelka–Munk theory [10], given as:

$$A_{\infty} = \frac{(1 - R_{\infty})^2}{2R_{\infty}} = \frac{K}{S} \quad (1)$$

Ciurczak et al. proved this relation for particles exceeding 85  $\mu\text{m}$  by analyzing aspirin, ascorbic acid,  $\text{Al}_2\text{O}_3$  and  $(\text{NH}_4)_3\text{PO}_4$  [11,12]. By using laser diffractometry as a reference method he found a negative linear correlation between NIR absorbance signal and reciprocal particle size at any wavelength. According to Ciurczak's theory, if the absorbance of two samples with different particle size, one having twice the diameter than the other, is measured, the absorbance of the larger sample is two times that of the smaller one [13]. Today data pretreatments, such as multiplicative scatter correction (MSC) for eliminating the particle size effects of NIR spectra, are well established and frequently applied. In recent publications different approaches for determining the samples particle size (particle diameter > 20  $\mu\text{m}$ ) with NIRS can be found, whereas all of them are based on Ciurczak's fundamental publications [11,12]. Ilari et al. performed a NIR particle size determination of NaCl, sorbitol and glass powder using PLS [14]. Frake et al. analyzed the particle size of an active ingredient in a lactose–monohydrate-matrix employing several chemometric approaches [15,16] while O'Neil et al. determined the particle sizes of aspirin, caffeine, paracetamol and microcrystalline cellulose [17,18]. Similar approaches were accomplished by Otsuka et al. [19,20], Reis et al. [21] and Huck and co-workers [22,23]. In all these investigations particles in the 100  $\mu\text{m}$  range and bigger were analyzed. Higgins et al. [24] described the NIRS based particle size analysis of smaller particles down to a  $D_{90}$  particle diameter of less than 250 nm. Here the theories based on Ciurczak's observations were inverted. The light path interacting with smaller particles is longer than in powders consisting of bigger particles, because the number of re-reflections between the particles increases. This finally results in a higher absorbance in samples of small particle size.

The aim of the present work is to demonstrate the applicability of NIRS as particle sizing method and to introduce an NIR approach for the identification and particle size determination of commercially available amoxicillin trihydrate bulk materials showing  $D_{90}$  particle diameters below 22  $\mu\text{m}$ .

## 2. Materials and methods

### 2.1. Materials

Amoxicillin trihydrate "BioChimica" was obtained from Applichem (Darmstadt, Germany). For diffuse reflection measurements quartz glass cells made of suprasil, type 20/C/1/0.5 (Starna, Pfungstadt, Germany) and type 540.111-QS (Hellma Optics, Jena, Germany) were used.

### 2.2. Sample preparation

The fractionation of fine powders (<50  $\mu\text{m}$ ) is generally difficult due to strong agglomeration tendency of the particles caused by interparticle forces. Dry methods would thus not be successful and the use of a dispersing medium is mandatory in order to overcome the agglomeration problem. In this work amoxicillin trihydrate bulk powder was fractionated by a wet fractionation method into 14 individual particle size fractions, whereas 11 fractions (1–11) were used to calibrate the NIR system (training set) and 3 fractions (A–C) were used as test set. The fractions were produced with the aid of nutsch filters by reducing the flow channel size stepwise. Diisopropylether with lecithin was used as suspending agent. The liquid was evaporated completely prior to NIR analysis and the drying process was monitored by observing characteristic absorption bands of the liquid as a function of time. Within 3 min the peaks of diisopropylether disappeared completely and the spectra collection was started.

### 2.3. Near-infrared-spectroscopy

A scanning polarization interferometer Fourier-transform NIR spectrometer (FT-NIR) (Büchi, Flawil, Switzerland) was used for spectra recording. The spectrometer is equipped with a tungsten-halogen lamp and a lead-sulfide detector temperate at 30 °C. The spectral resolution is 12  $\text{cm}^{-1}$  with an absolute wavelength accuracy of  $\pm 2 \text{cm}^{-1}$  and a relative reproducibility of 0.5  $\text{cm}^{-1}$  between 4000 and 10,000  $\text{cm}^{-1}$  (2500–1000 nm). A coupled sample desk (SD 1086, Büchi) was used to probe the samples. One spectrum represents the average of 13 scans. Each sample was measured 5 times independently at which no differences between the different spectra of the same sample could be observed. Prior to developing any calibration model the measurement parameters, e.g. choice of the suspending agent, composition of the suspensions, number of scans, choice of the best suitable cell, were tested and optimized. For recording the spectra and the application of PCA-algorithms NIRCAL 4.21/Build 389 software (Büchi) was used. PLS and PCR calibration models were generated with The Unscrambler 9.6 (Camo, Oslo, Norway). All calibrations were validated using systematic cross validation (5 samples per segment). For quantification different regression models were established, evaluated and compared. In addition to cross validation independent test-samples (or "unknown" samples) were predicted by the models, considering the following statistical parameters:

- (1) BIAS is the average deviation between predicted values ( $y_i$ ) and reference values ( $x_i$ ). In the calibration set the BIAS is 0.

$$\text{BIAS} = \frac{\sum_{i=1}^n (x_i - y_i)}{n} \quad (2)$$

- (2) Standard error of prediction (SEP) is defined as the standard deviation of differences between reference values and NIRS-results in the validation set.

$$\text{SEP} = \sqrt{\frac{\sum_{i=1}^n (x_i - y_i - \text{BIAS})^2}{n - 1}} \quad (3)$$

- (3) Standard error of calibration (SEC) is describes as the standard deviation of differences between reference values and NIRS-results in the calibration set.

$$\text{SEC} = \sqrt{\frac{\sum_{i=1}^n (x_i - y_i - \text{BIAS})^2}{n - 1}} \quad (4)$$

- (4) Squared correlation coefficient  $r^2$ : for evaluating the difference between reference and measures values.

**Table 1**  
Results from reference measurements. Values in brackets show the variations.

| Sample | D10 particle diameter ( $\mu\text{m}$ ) | D50 particle diameter ( $\mu\text{m}$ ) | D90 particle diameter ( $\mu\text{m}$ ) |
|--------|---|---|---|
| 1      | 2.5 (0.1)                               | 6.3 (0.1)                               | 18.0 (0.6)                              |
| 2      | 2.6 (0.0)                               | 8.9 (0.5)                               | 21.7 (1.1)                              |
| 3      | 1.8 (0.1)                               | 4.5 (0.1)                               | 10.8 (0.1)                              |
| 4      | 2.3 (0.1)                               | 5.6 (0.0)                               | 14.4 (0.0)                              |
| 5      | 2.5 (0.1)                               | 6.3 (0.1)                               | 15.8 (0.3)                              |
| 6      | 1.8 (0.0)                               | 4.5 (0.3)                               | 11.2 (1.3)                              |
| 7      | 1.9 (0.1)                               | 5.1 (0.0)                               | 12.7 (0.4)                              |
| 8      | 1.8 (0.0)                               | 4.2 (0.0)                               | 10.5 (0.1)                              |
| 9      | 1.7 (0.0)                               | 4.2 (0.3)                               | 11.5 (0.6)                              |
| 10     | 1.6 (0.0)                               | 3.4 (0.1)                               | 6.9 (0.2)                               |
| 11     | 1.6 (0.0)                               | 3.5 (0.1)                               | 8.4 (0.3)                               |
| A      | 2.0 (0.4)                               | 4.3 (0.3)                               | 18.7 (1.6)                              |
| B      | 2.4 (0.1)                               | 4.5 (0.5)                               | 14.4 (0.5)                              |
| C      | 2.5 (0.0)                               | 4.7 (0.3)                               | 13.3 (1.4)                              |

#### 2.4. Image analysis

Microscopic image analysis was chosen for particle size determination because the sample amount of the individual size fractions was rather small (<100 mg). A Carl Zeiss Axioplan microscope with a Carl Zeiss Neofluar 20 $\times$  PH2 objective (Carl Zeiss, Oberkochen, Germany) in combination with a Märzhäuser stage (Märzhäuser, Wetzlar, Germany), an Olympus F-View II camera (Olympus Austria GesmbH, Vienna) and the Olympus Cell\*F Software (Version 2.5) was used. One droplet of a sample suspension (0.1% lecithin in diisopropylether; 5 s sonication) was prepared with one droplet of paraffinum liquidum (Ph. Eur.) on a microscope slide. The image analysis (IA) was performed on an array of 10  $\times$  10 images, detecting and evaluating all particles with a minimum area of 10 pixels. The “average particle diameter” was used to characterize the particle dimensions, which is the mean distance between two points on the perimeter of a particle, measured every degree (1–179 $^\circ$ ). This particle diameter is a statistical feature extracted from the boundary function of the whole particle profile. Every sample was measured twice. Table 1 shows the statistics of the particle size distributions for all samples. The D10, D50 and D90 values indicate the maximal particle size diameter that includes 10%, 50% and 90% of the particles, respectively (number-weighted basis). For example the D90 value means that 90% of the particles are smaller than this particle diameter whereas the remaining 10% of the particles are larger.

### 3. Results and discussion

One of the crucial points when establishing a stable calibration of amoxicillin trihydrate, was to separate the powder into representative particle size fractions before conducting the reference measurements. The particle size distributions of the obtained size

**Table 2**  
Allocation of vibrations with consideration of the chemical structure of amoxicillin.

| Wavenumber ( $\text{cm}^{-1}$ ) | Vibrational mode                                  |
|---------------------------------|---|
| 4080, 4152                      | $\nu_{\text{as}}$ (C–H arom.) + $\nu$ (C–C arom.) |
| 4224, 4260                      | $\nu$ (C–H arom.) + $\delta$ (C–H arom.)          |
| 4320                            | $\nu$ (N–H) + $\delta$ (C–H)                      |
| 4392                            | $\nu$ (O–H) + $\nu$ (C–C arom.)                   |
| 4572                            | $\nu$ (C–H) + $\nu$ (C=O)                         |
| 4644                            | 2 $\times$ Amide I + amide III                    |
| 4728                            | $\nu_{\text{s}}$ (N–H) + amide III                |
| 4800                            | $\nu$ (O–H) + $\delta$ (C–H)                      |
| 5136                            | $\nu$ (O–H) + $\delta$ (C–H)                      |
| 5460–6120                       | 2 $\times$ $\nu$ (C–H)                            |
| 6840                            | 2 $\times$ $\nu$ (N–H)                            |
| 7212–7464                       | 2 $\times$ $\nu$ (N–H) + $\delta$ (C–H)           |
| 8268–8688                       | 3 $\times$ $\delta$ (C–H)                         |

fractions are in the same range as in the samples in Higgins' study obtained by milling [24].

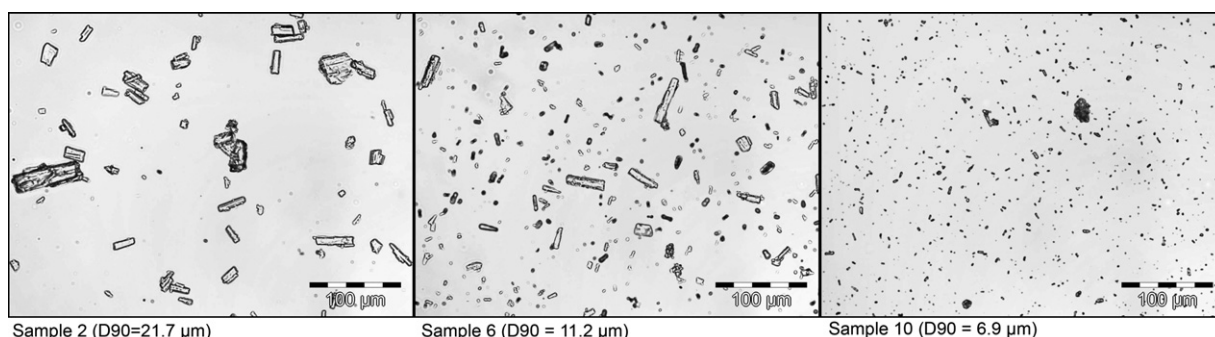
Image analysis was used as reference method while cross validated PLS and PCR algorithms were applied and compared to achieve a robust and representative calibration model. Fig. 2 shows the light microscope photography of three exemplary after fractionation, representing sample 2 (D90 = 21.7  $\mu\text{m}$ ), sample 6 (D90 = 11.2  $\mu\text{m}$ ) and sample 10 (D90 = 6.9  $\mu\text{m}$ ). In addition, test-samples (samples A–C) were subjected to the models to proof its prediction ability in practice on real samples.

#### 3.1. Qualitative analysis – identification of the chemical and solid state form

Characteristic absorption bands, indicating specific molecular vibrations of the amoxicillin trihydrate, observed in the NIR spectra are summarized in Table 2. Preferentially characteristic overtones and combination vibrations can be seen in the NIR spectrum. The rather sharp bands can be used to identify amoxicillin trihydrate by comparison with data obtained from spectral libraries (Spectrum Search Plus, Perkin Elmer, Rodgau, Germany). Therefore, it is also possible to differentiate amoxicillin trihydrate from other  $\beta$ -lactam antibiotics such as ampicillin trihydrate, where the only difference to amoxicillin trihydrate is one missing OH-group. Furthermore the NIR-spectrum allows in most cases also a clear identification of the solid state form of the compound (polymorphs, solvates, hydrates, amorphous form) which is well documented in the literature [25–28].

#### 3.2. Correlation between absorbance and particle size

As shown in Fig. 3, the main effect of particle size variations on NIR-spectra is a baseline offset. Interestingly, the well-known phenomenon that larger particles show a stronger light absorption than smaller ones cannot be observed here. Ciurczak and co-workers

**Fig. 2.** Light-optical microscope images of sample 2, sample 6 and sample 10.

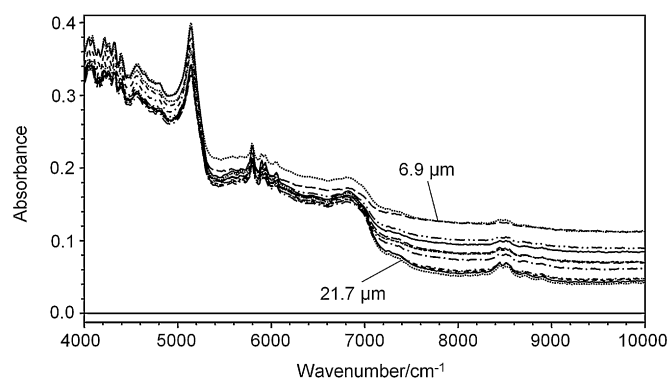


**Fig. 3.** NIR spectra of amoxicillin trihydrate with D90 particle diameter ranging from 6.9 to 21.7  $\mu\text{m}$ .

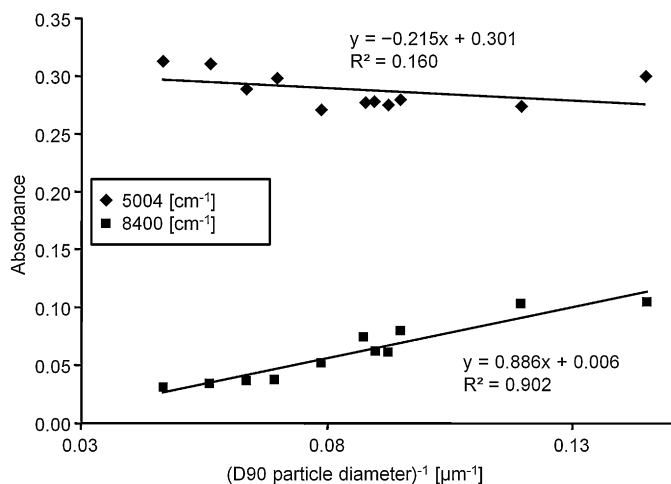


**Fig. 4.** Correlation between absorbance and reciprocal D90 particle diameter at specific wavenumbers.

proved a negative linear relation between absorbance and reciprocal particle size [11] based on the Kubelka–Munk theory for particles  $>85 \mu\text{m}$ . Operating in a particle size range  $<85 \mu\text{m}$ , like in our case, the opposite effect was observed, meaning that smaller particles show higher absorbance than larger ones. Similar observations were made by Higgins et al. [24]. As shown in Table 3, a correlation between particle size and absorbance can be seen exclusively at higher wavenumbers. There is an obvious correlation between the reciprocal particle diameter and the absorbance signal – noticeable for wavenumbers  $>7000 \text{ cm}^{-1}$ , indicated by high regression coefficients (Fig. 4). At low wavenumbers ( $5004 \text{ cm}^{-1}$ )

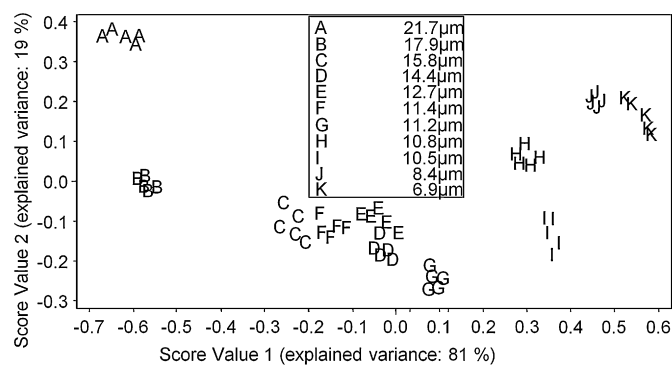


**Fig. 5.** Score plot showing score value 1 against score value 2 ( $6996\text{--}9996 \text{ cm}^{-1}$ ).

only a very low  $R^2$  of 0.160 was obtained at generally less baseline shift, whereas at high wavenumbers ( $8004 \text{ cm}^{-1}$ ) the  $R^2$  value is 0.902. A plausible explanation for the increasing absorbance with decreasing particle size was given by Higgins et al. [24]. Larger particles produce more backscattered light, resulting in a lower overall absorption of the NIR-spectrum. In powders with smaller particles less light is directly scattered back to the detector and the dispersed light rays undergo a greater multiple scattering between the particles before they are reflected back to the detector. The increased path lengths in samples with small particle size also result in a higher absorption of the NIR light.

### 3.3. Principal component analysis (PCA)

After  $\log(1/R)$  transforming the reflection spectra a PCA was performed. As mentioned before no additional pretreatments were utilized, even smoothing was not necessary due to an acceptable signal-noise-ratio throughout the whole wavenumber range. Observing the absorptions of the different sized samples at certain wavenumbers, in the regions  $>7000 \text{ cm}^{-1}$  the highest coherence could be observed. This finding combined with the linear correlation between absorbance and reciprocal particle size lead to the attempt to perform multivariate data analysis by implementing a limited wavenumber region. The PCA was performed from  $4008$  to  $9996 \text{ cm}^{-1}$  and from  $6996$  to  $9996 \text{ cm}^{-1}$ . The second spectral range leads to slightly better classification of the samples with different particle sizes, indicating that the particle size effects are more pronounced in the higher wavenumber region of the spectra. The particle size is entirely described through the first factor, as can be seen from the score plot in Fig. 5. Along score value 1 the D90 particle diameter decreases constantly as the score value increases.

**Table 3**  
D90 particle diameter and absorbances at certain wavenumbers.

| Sample | D90 particle diameter ( $\mu\text{m}$ ) | Absorbance             |                        |                        |                        |                        |
|--------|---|------------------------|------------------------|------------------------|------------------------|------------------------|
|        |   | $5004 \text{ cm}^{-1}$ | $6000 \text{ cm}^{-1}$ | $6996 \text{ cm}^{-1}$ | $8004 \text{ cm}^{-1}$ | $9000 \text{ cm}^{-1}$ |
| 10     | 6.9                                     | 0.2955                 | 0.2057                 | 0.1722                 | 0.1240                 | 0.1157                 |
| 11     | 8.4                                     | 0.2691                 | 0.1894                 | 0.1603                 | 0.1239                 | 0.1163                 |
| 8      | 10.5                                    | 0.2746                 | 0.1833                 | 0.1503                 | 0.1007                 | 0.0927                 |
| 3      | 10.8                                    | 0.2709                 | 0.1746                 | 0.1391                 | 0.0820                 | 0.0741                 |
| 6      | 11.2                                    | 0.2735                 | 0.1787                 | 0.1432                 | 0.0825                 | 0.0735                 |
| 9      | 11.4                                    | 0.2718                 | 0.1796                 | 0.1464                 | 0.0944                 | 0.0872                 |
| 7      | 12.7                                    | 0.2668                 | 0.1716                 | 0.1363                 | 0.0733                 | 0.0648                 |
| 4      | 14.4                                    | 0.2938                 | 0.1805                 | 0.1380                 | 0.0568                 | 0.0484                 |
| 5      | 15.8                                    | 0.2851                 | 0.1758                 | 0.1352                 | 0.0580                 | 0.0500                 |
| 1      | 17.9                                    | 0.3061                 | 0.1877                 | 0.1430                 | 0.0545                 | 0.0451                 |
| 2      | 21.7                                    | 0.3081                 | 0.1847                 | 0.1399                 | 0.0512                 | 0.0426                 |

**Table 4**  
Comparison of parameters indicating the quality of a calibration.

| Calibration model                 | Number of factors | $r^2$ (cal.) | SEP  | SEC  | BIAS (val.) |
|-----------------------------------|-------------------|--------------|------|------|-------------|
| PLS (6996–9996 $\text{cm}^{-1}$ ) | 2                 | 0.933        | 1.61 | 1.50 | 0.00276     |
| PLS (4008–9996 $\text{cm}^{-1}$ ) | 2                 | 0.939        | 1.55 | 1.43 | 0.00438     |
| PCR (6996–9996 $\text{cm}^{-1}$ ) | 2                 | 0.930        | 1.63 | 1.53 | 0.00126     |
| PCR (4008–9996 $\text{cm}^{-1}$ ) | 2                 | 0.939        | 1.55 | 1.43 | 0.00461     |

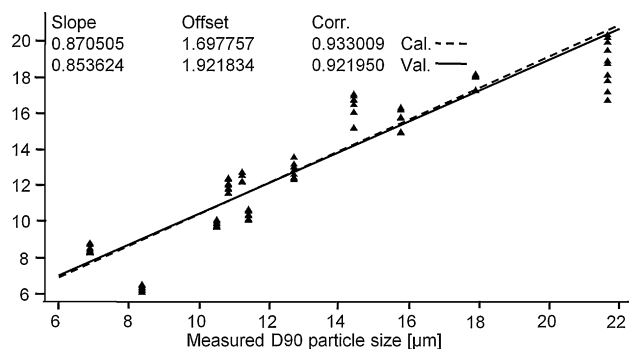


**Fig. 6.** PLS calibration for  $D_{90}$  particle diameter.

### 3.4. Quantitative analysis

For determining the  $D_{90}$  particle diameter partial least squares regression (PLSR) and principal component regression (PCR) were performed. PCR is based on PCA followed by multiple linear regressions (MLR). When performing PLS, from the beginning the property of interest (e.g. particle size) is integrated in the calculation of the PCA as an individual concentration matrix. In a first step the  $D_{90}$  particle diameter was calibrated by PLS and validated by cross validation, taking a range from 6996 to 9996  $\text{cm}^{-1}$  into consideration. Two factors were found to sufficiently describe the variance in the spectra. Further performed PCR modeling in a range from 6996 to 9996  $\text{cm}^{-1}$  and 4008 to 9996  $\text{cm}^{-1}$  and PLS from 4008 to 9996  $\text{cm}^{-1}$  also resulted in two factors to describe the variance. The samples T1, T2 and T3 were taken as independent, “unknown” samples to test the prediction ability of the models. As can be seen in Fig. 6,  $D_{90}$  particle size can be predicted with high accuracy. The corresponding statistical parameters are summarized in Table 4. All performed calibration models lead to similar, low SEPs, SECs and BIAs and high regression coefficients. The “unknown” samples were predicted using PLS from 6996 to 9996  $\text{cm}^{-1}$  and the  $D_{90}$  particle diameter could be predicted with accuracy between 0.14 and 1.70% (Fig. 7).

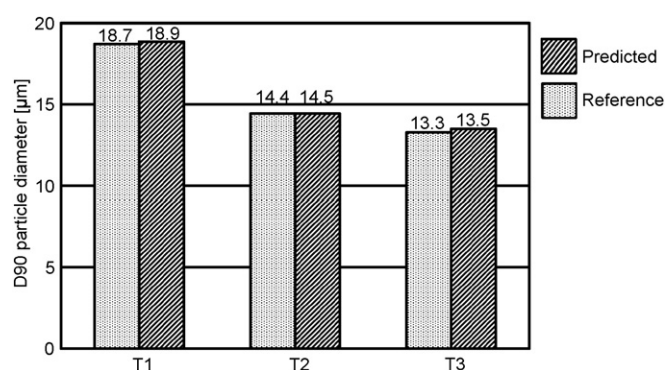


**Fig. 7.** Predicted  $D_{90}$  particle diameter (PLS, 6996–9996  $\text{cm}^{-1}$ ) vs. measured  $D_{90}$  particle diameter.

## 4. Conclusions

This study demonstrates the applicability of NIR diffuse reflection spectroscopy in combination with multivariate data analysis to determine  $D_{90}$  particle size of amoxicillin trihydrate bulk materials, with a minimal expenditure in sample preparation. By fractionating the particles robust qualitative (PCA) and quantitative (PCR, PLS) models were established showing high linearity between absorbance and reciprocal particle diameter of amoxicillin trihydrate in a certain wavenumber range. The spectra of the observed particle range of 7–22  $\mu\text{m}$  ( $D_{90}$ ) show an inverse relationship between absorbance (baseline offset) and particle size, similar to the study of Higgins et al. [24] who analyzed nanoparticle samples ( $D_{90} < 230 \text{ nm}$ ). This observation suggests that the characteristics of the NIR-absorbance of small particles is contradictory to the theories of Ciurczak et al. [11,12], who focused on particle size ranges bigger than 85  $\mu\text{m}$ . However, the observation that the baseline offset increases with decreasing particle size was also observed in a recent study by Abebe et al. [25]. In summary, the present study demonstrates again that NIR spectroscopy can be successfully applied as a fast and robust non-invasive method for particle size analysis. The main advantages of this method are the high automation potential and the simultaneous acquisition of the identity (chemical and crystal form) and the average particle size of a sample, which highly qualifies the method for the quality control of pharmaceutical raw materials (active ingredients and excipients). However, NIR-spectroscopy cannot be regarded as a replacement for standard particle sizing methods such as laser diffraction, as it provides only an average number for the particle size characteristics and no information about particle size distribution or specific particle shape features.

## Acknowledgement

For financial support we thank the Leopold-Franzens University, Innsbruck, Austria (Nachwuchsförderung).

## References

- [1] H. Leuenberger, M. Lanz, Pharmaceutical powder technology – from art to science: the challenge of the FDA’s process analytical technology initiative, *Adv. Powder Technol.* 16 (2005) 3–25.
- [2] J.N. Miller, J.C. Miller, *Statistics and Chemometrics for Analytical Chemistry*, Prentice Hall PTR, Harlow, 2005.
- [3] J. Einax, H.W. Zwaninger, S. Geiss, *Chemometrics in Environmental Analysis*, Wiley-VCH, Weinheim, 1997.
- [4] H.W. Siesler, Y. Ozaki, S. Kawata, H.M. Heise, *Near-Infrared Spectroscopy*, Wiley-VCH, Weinheim, 2002.
- [5] K.H. Esbensen, D. Guyot, F. Westad, L.P. Houmøller, *Multivariate Data Analysis: In Practice: An Introduction to Multivariate Data Analysis and Experimental Design*, Camo, Oslo, 2002.
- [6] R. DiFoggio, Examination of some misconceptions about near-infrared analysis, *Appl. Spectrosc.* 49 (1995) 67–75.
- [7] H.C. van de Hulst, *Light Scattering by Small Particles*, Dover Publications, Mineola, 1981.
- [8] E.W. Ciurczak, J.K. Drennen, *Pharmaceutical and medical applications of near-infrared spectroscopy*, CRC, New York, 2002.
- [9] P. Kubelka, New contributions to the optics of intensely light-scattering materials. Part I, *J. Opt. Soc. Am.* 38 (1948) 448–457.
- [10] P. Kubelka, F. Munk, An article on optics of paint layers, *Z. Tech. Phys.* 12 (1931) 593–601.

- [11] E.W. Ciurczak, R.P. Torlini, M.P. Demkowicz, Determination of particle size of pharmaceutical raw materials using near-infrared reflectance spectroscopy, *Spectroscopy* 1 (1986) 36–39.
- [12] E. Ciurczak, Uses of near-infrared spectroscopy in pharmaceutical analysis, *Appl. Spectrosc. Rev.* 23 (1987) 147–163.
- [13] D.J. Dahm, K.D. Dahm, *Interpreting Diffuse Reflectance and Transmittance*, NIR Publications, Chichester, 2007.
- [14] J.L. Ilari, H. Martens, T. Isaksson, Determination of particle size in powders by scatter correction in diffuse near-infrared reflectance, *Appl. Spectrosc.* 42 (1988) 722–728.
- [15] P. Frake, C.N. Luscombe, D.R. Rudd, I. Gill, J. Waterhouse, U.A. Jayasooriya, Near-infrared mass median particle size determination of lactose monohydrate, evaluating several chemometric approaches, *Analyst* 123 (1998) 2043–2046.
- [16] P. Frake, C.N. Luscombe, D.R. Rudd, J. Waterhouse, U.A. Jayasooriya, Mass median particle size determination of an active compound in a binary mixture using near-infrared spectroscopy, *Anal. Commun.* 35 (1998) 133–134.
- [17] A.J. O'Neil, R.D. Jee, A.C. Moffat, The application of multiple linear regression to the measurement of the median particle size of drugs and pharmaceutical excipients by near-infrared spectroscopy, *Analyst* 123 (1998) 2297–2302.
- [18] A.J. O'Neil, R.D. Jee, A.C. Moffat, Measurement of the cumulative particle size distribution of microcrystalline cellulose using near infrared reflectance spectroscopy, *Analyst* 124 (1999) 33–36.
- [19] M. Otsuka, Y. Mouri, Y. Matsuda, Chemometric evaluation of pharmaceutical properties of antipyrine granules by near-infrared spectroscopy, *AAPS Pharm-SciTech* 4 (2003) 142–148.
- [20] M. Otsuka, Comparative particle size determination of phenacetin bulk powder by using Kubelka–Munk theory and principal component regression analysis based on near-infrared spectroscopy, *Powder Technol.* 141 (2004) 244–250.
- [21] M.M. Reis, P.H.H. Araújo, C. Sayer, R. Giudici, Correlation between polymer particle size and in situ NIR spectra, *Macromol. Rapid Commun.* 24 (2003) 620–624.
- [22] C.W. Huck, N. Heigl, M. Najam-ul-Haq, M. Rainer, R.M. Vallant, G.K. Bonn, Progress in silica chemistry—determination of physico-chemical parameters via near-infrared diffuse reflection spectroscopy, *Open Anal. Chem. J.* 1 (2007) 21–27.
- [23] N. Heigl, C.H. Petter, M. Lieb, G.K. Bonn, C.W. Huck, Near-infrared reflection spectroscopy and partial least squares regression for determining the total carbon coverage of silica packings for liquid chromatography, *Vib. Spectrosc.* 49 (2009) 155–161.
- [24] J.P. Higgins, S.M. Arrivo, G. Thurau, R.L. Green, W. Bowen, A. Lange, A.C. Templeton, D.L. Thomas, R.A. Reed, Spectroscopic approach for on-line monitoring of particle size during the processing of pharmaceutical nanoparticles, *Anal. Chem.* 75 (2003) 1777–1785.
- [25] S.B. Abebe, X.Z. Wang, R. Li, K.J. Roberts, X. Lai, The information content in NIR spectral data for slurries of organic crystals, *Powder Technol.* 179 (2008) 176–183.
- [26] U.J. Griesser, J. Stowell, Solid state analysis and polymorphism, in: D.C. Lee, M. Webb (Eds.), *Pharmaceutical Analysis*, Blackwell Publishing, Oxford, 2003, pp. 240–294.
- [27] M. Blanco, D. Valdes, M.S. Bayod, F. Fernandez-Mari, I. Llorente, Characterization and analysis of polymorphs by near-infrared spectrometry, *Anal. Chim. Acta* 502 (2004) 221–227.
- [28] M. Blanco, M. Alcalá, J.M. González, E. Torras, Near infrared spectroscopy in the study of polymorphic transformations, *Anal. Chim. Acta* 567 (2006) 262–268.